Inorg. Chem. **2003**, *42*, 2440–2446

Determination of Ligand-Field Parameters and f-Electronic Structures of Double-Decker Bis(phthalocyaninato)lanthanide Complexes

Naoto Ishikawa,* Miki Sugita, Tomoko Okubo, Naohiro Tanaka, Tomochika Iino, and Youkoh Kaizu*

Department of Chemistry, Tokyo Institute of Technology, O-okayama, Meguro-ku, Tokyo 152-8551, Japan

Received December 22, 2002

The f-electronic structures of the ground states of anionic bis(phthalocyaninato)lanthanides, $[Pc_2Ln]^-$ (Pc = dianion of phthalocyanine, Ln = Tb^{3+}, Dy^{3+}, Ho^{3+}, Er^{3+}, Tm^{3+}, or Yb^{3+}), are determined. Magnetic susceptibilities of the powder samples of $[Pc_2Ln]$TBA (TBA = tetra-*n*-butylammonium cation) in the range 1.8–300 K showed characteristic temperature dependences which resulted from splittings of the ground-state multiplets. NMR signals for the two kinds of protons on the Pc rings at room temperature were shifted to lower frequency with respect to the diamagnetic Y complex in Ln = Tb, Dy, and Ho cases, and to higher frequency in Er, Tm, and Yb cases. The ratios of the paramagnetic shifts of the two positions were near constant in the six cases. This indicates that the shifts are predominantly caused by the magnetic dipolar term, which is determined by the anisotropy of the magnetic susceptibility of the lanthanide ion. Using a multidimensional nonlinear minimization algorithm, we determined a set of ligand-field parameters that reproduces both the NMR and the magnetic susceptibility data of the six complexes simultaneously. Each ligand-field parameter was assumed to be a linear function of atomic number of the lanthanide. The energies and wave functions of the sublevels of the multiplets are presented. Temperature dependences of anisotropies in the magnetic susceptibilities are theoretically predicted for the six complexes.

Introduction

Information on multiplet splitting in a 4f-electronic system is of crucial importance for studying and understanding magnetic properties of a lanthanide complex. The temperature dependence of magnetic susceptibility, for example, is determined by how the sublevels in the ground-state multiplet are thermally populated as a function of temperature. Determination of the sublevel structure is, however, a difficult task both experimentally and theoretically in many cases.

The f-electrons in most of lanthanide complexes are considered to have properties which are close to those of isolated ions. The energies of ground- and excited-state multiplets are determined by *LS*-coupling in which total angular momentum *J* is the good quantum number for each state. The energies of the f−f electronic spectral bands in the region from near-IR to UV, if they are available, are similar to those of free ions. Fine structure in each band is ascribed to ligand-field splitting of the ground- and excited-state multiplet. In fortunate cases where the fine structures are sharp enough to separate from each other, it is possible to obtain direct information on the energy levels of the substates within a multiplet, and ligand-field (LF) parameters can be determined. Otherwise, however, sublevel structures cannot be obtained by this approach.

Recently, Ishikawa et al. proposed a new method to determine electronic structures of a series of isostructural lanthanide complexes.[1] In this method, each ligand-field parameter is assumed to be a linear function of the atomic number. Under this restriction, a multidimensional nonlinear minimization algorithm is employed to search the set of LF parameters which simultaneously reproduces both paramagnetic shifts of ^{1}H NMR spectra and temperature dependence of magnetic susceptibilities. As the first application of this method, the ligand-field parameters were determined for a series of dinuclear lanthanide complexes with phthalocyanine.[1] With the knowledge of sublevel structures of individual f-systems in the dinuclear complexes, the study of interaction between f-electronic systems was carried out.[2] This was the first study of f−f interaction in dinuclear lanthanide complexes based on precise LF parameters.

* To whom correspondence should be addressed. E-mail: ishikawa@chem.titech.ac.jp (N.I.).

(1) Ishikawa, N.; Iino, T.; Kaizu, Y. *J. Phys. Chem. A* **2002**, *106*, 9543.
(2) Ishikawa, N.; Iino, T.; Kaizu, Y. *J. Am. Chem. Soc.* **2002**, *124*, 11440.

10.1021/ic026295u CCC: $25.00
Published on Web 03/11/2003

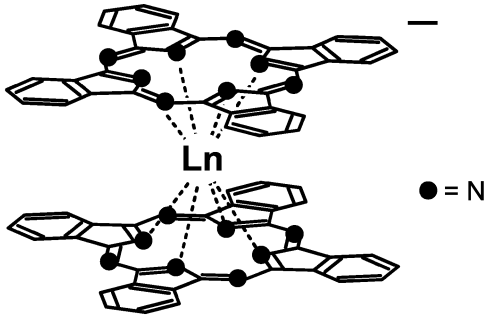

Figure 1. Schematic diagram of $[Pc_2Ln]^-$ (Ln = Tb, Dy, Ho, Er, Tm, or Yb).

This paper presents the first determination of the sublevel structures and ligand-field parameters of the series of the "double-decker" phthalocyanine complexes (Figure 1), which consist of two π-conjugate planar ligands and one of the following trivalent ions, Tb^{3+}, Dy^{3+}, Ho^{3+}, Er^{3+}, Tm^{3+}, and Yb^{3+}. Neither fluorescence nor absorption spectra associated with lanthanide centers are obtainable in these complexes, because of the low-lying Pc-centered energy levels quenching the lanthanide fluorescence, and the extremely intense Pc-centered absorption bands concealing the lanthanide-centered bands.

The phthalocyanine double-decker complexes have been known to exist in several oxidation states.[3−6] Two oxidation states, $[Pc_2Ln^{III}]^-$ and $[Pc_2Ln^{III}]^0$ (Pc = dianion of phthalocyanine), are stable in air. In the former oxidation state, each Pc ligand has a formal charge of −2 with a closed shell electronic configuration. The present paper concerns this oxidation state. The information on the f-electronic structures presented here is also essential for future study of the latter oxidized form, which has a π-hole delocalized over two ligands.[7] Although there are a few reports on magnetic interaction between the f-system and the π-hole,[8−10] precise descriptions of the electronic states and nature of the interaction are still unknown, since there has been no study on the sublevel structure of the multiplets.

Each lanthanide ion is 8-fold coordinated by the pyrrole nitrogen atoms of the two Pc ligands. The X-ray study for $[Pc_2Ln]$TBA (Ln = Lu, Ho, and Gd; TBA = tetra-*n*-butylammonium cation) has shown that in the complex with the smallest ion with f^{14}-configuration, Lu^{3+}, the skew angle the two ligands make is 45.0°, and the ligand field is approximately of D_{4d} symmetry.[11] The angle gradually becomes smaller with a decrease of the atomic number of the lanthanide ion. The distance between the two ligands regularly decreases as the lanthanide atomic number increases and is correlated with the change of ionic radii due to the lanthanide contraction.

The sandwich-type complexes have the most basic structure of "stacked π-conjugate molecules", and their spectroscopic and electrochemical properties[4] have been studied in terms of $\pi-\pi$ interactions between adjacent ligands.[12,13] In the perspective as "stacked π-conjugate molecules", the lanthanide ions inserted between the ligands have been treated as a "bridge", the length of which is determined by the ionic radii regularly varying through the lanthanide series. Although the importance of the role of the f-electrons has been mentioned occasionally, there has been no decisive study on it. The study presented here is the first attempt to shed light on the sublevel structures of the f-electronic systems of the double-decker complexes.

Experimental Section

The powder samples of $[Pc_2Ln]$TBA (Ln = Tb, Dy, Ho, Er, Tm, or Yb) were prepared by a conventional method.[14,15] Magnetic susceptibility measurements were carried out on a Quantum Design MPMS-5 SQUID (superconducting quantum interference device) magnetometer. The corresponding experimental data for $[Pc_2Y]$-TBA were used to correct for the diamagnetic susceptibility contribution in each the sample. ^{1}H NMR spectra of the complexes were measured in CD_3CN solution at 27 °C with $(CH_3)_4Si$ as an internal standard on a JEOL Lambda-300 NMR spectrometer.

Results

SQUID Measurements. Figure 2 shows the plots of molar magnetic susceptibility times temperature ($\chi_m T$) against temperature T for the powder samples of $[Pc_2Tb]$TBA, $[Pc_2Dy]$TBA, and $[Pc_2Ho]$TBA. As temperature rises, $\chi_m T$ asymptotically approaches the corresponding value of a free trivalent ion in each case: $\chi_m T = 11.81$ emu K/mol for Tb^{3+}, 14.18 emu K/mol for Dy^{3+}, and 14.07 emu K/mol for Ho^{3+}. With lowering temperature, the $\chi_m T$ value of $[Pc_2Tb]$TBA gradually decreases. After reaching the minimum (10.3 emu K/mol) at 11 K, the $\chi_m T$ value slightly increases and reaches 10.5 emu K/mol at 2.0 K. $[Pc_2Dy]$TBA shows a monotonic decrease in $\chi_m T$ with lowering temperature. The value reaches 10.2 emu K/mol at 2 K. $[Pc_2Ho]$TBA shows a similar tendency, but with a greater decrease: $\chi_m T$ is 6.3 emu K/mol at 2 K.

Figure 3 shows the $\chi_m T$ versus T plots of $[Pc_2Er]$TBA, $[Pc_2Tm]$TBA, and $[Pc_2Yb]$TBA. Again, the curves approach the $\chi_m T$ value of a free Er^{3+} (11.48 emu K/mol), Tm^{3+} (7.15 emu K/mol), and Yb^{3+} (2.57 emu K/mol), respectively, at room temperature. With lowering temperature, $\chi_m T$ decreases monotonically in all three cases, in different manners. The

(3) Riou, M. T.; Clarisse, C. *J. Electroanal. Chem.* **1989**, *274*, 107.
(4) Konami, H.; Hatano, M.; Kobayashi, N.; Osa, T. *Chem. Phys. Lett.* **1990**, *165*, 397.
(5) Iwase, H.; Harnoode, C.; Kameda, Y. *J. Alloys Compd.* **1993**, *134*, 280.
(6) Harnoode, C.; Takamura, K.; Kubota, H.; Sho, K.; Fujisawa, K.; Kitamura, F.; Ohsaka, T.; Tokuda, K. *Electrochemistry* **1999**, *67*, 832.
(7) Ishikawa, N.; Ohno, O.; Kaizu, Y. *Chem. Phys. Lett.* **1991**, *180*, 51.
(8) Padilla, J.; Hatfield, W. E. *Synth. Met.* **1989**, *29*, F45.
(9) Trojan, K. L.; Hatfield, W. E.; Kepler, K. D.; Kirk, M. L. *J. Appl. Phys.* **1991**, *69*, 6007.
(10) Trojan, K. L.; Kendall, J. L.; Kepler, K. D.; Hatfield, W. E. *Inorg. Chim. Acta* **1992**, *198−200*, 795.
(11) Koike, N.; Uekusa, H.; Ohashi, Y.; Harnoode, C.; Kitamura, F.; Ohsaka, T.; Tokuda, K. *Inorg. Chem.* **1996**, *35*, 5798.
(12) (a) Ishikawa, N.; Ohno, O.; Kaizu, Y.; Kobayashi, H. *J. Phys. Chem.* **1992**, *96*, 8832. (b) Ishikawa, N.; Ohno, O.; Kaizu, Y. *J. Phys. Chem.* **1993**, *97*, 1004. (c) Ishikawa, N.; Kaizu, Y. *Chem. Phys. Lett.* **1994**, *228*, 625.
(13) (a) Ishikawa, N.; Kaizu, Y. *J. Porphyrins Phthalocyanines* **1999**, *3*, 514. (b) Ishikawa, N. *J. Porphyrins Phthalocyanines* **2001**, *5*, 87.
(14) De Cian, A.; Moussavi, M.; Fischer, J.; Weiss, R. *Inorg. Chem.* **1985**, *24*, 3162.
(15) Konami, H.; Hatano, M.; Tajiri, A. *Chem. Phys. Lett.* **1989**, *160*, 163.

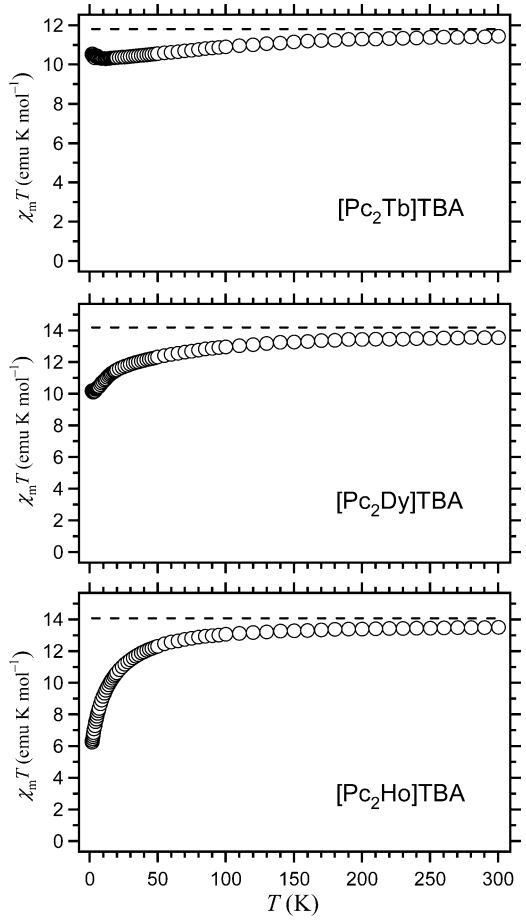

Figure 2. Plots of $\chi_m T$ against temperature T for [Pc_2Tb]TBA (top), [Pc_2Dy]TBA (center), and [Pc_2Ho]TBA (bottom). Each dashed line is the $\chi_M T$ value of the corresponding free lanthanide ion.

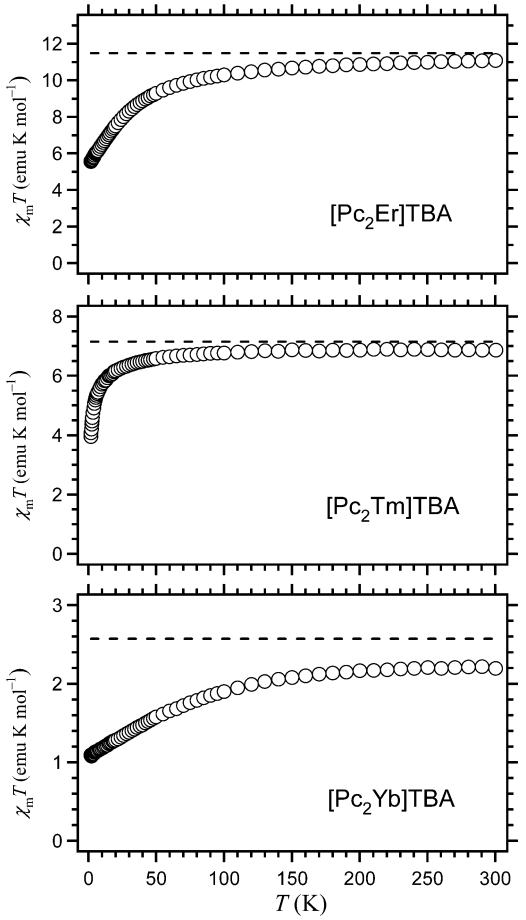

Figure 3. Plots of $\chi_m T$ against temperature T for [Pc_2Er]TBA (top), [Pc_2Tm]TBA (center), and [Pc_2Yb]TBA (bottom). Each dashed line is the $\chi_M T$ value of the corresponding free lanthanide ion.

$\chi_m T$ values of [Pc_2Er]TBA, [Pc_2Tm]TBA, and [Pc_2Yb]TBA at 2 K are 5.6, 4.1, and 1.1 emu K/mol, respectively.

^{1}H NMR Measurements. The assignments of ^{1}H NMR signals and paramagnetic shifts of [Pc_2Ln]$^-$ are summarized in Table 1. The paramagnetic shift $\Delta\delta$ in the present work is defined as the deviation of a chemical shift δ of a paramagnetic species from that of diamagnetic [Pc_2Y]TBA. The complexes have two different kinds of protons on the Pc rings. The protons near and far from the center will be referred to as α and β, respectively. The signals in [Pc_2Y]-TBA are observed at 8.84 ppm for the α position, and 8.13 ppm for the β position. The largest paramagnetic shifts are observed in [Pc_2Tb]TBA. In the Ln = Tb, Dy, and Ho cases, the $\Delta\delta$ values are negative. The absolute value of $\Delta\delta$ reduces as the atomic number increases. The direction of the shift reverses in the Ln = Er, Tm, and Yb cases. [Pc_2Er]TBA and [Pc_2Tm]TBA have similar $\Delta\delta$ values. [Pc_2Yb]TBA exhibits the smallest $|\Delta\delta|$ values in the six cases.

Throughout the series, the ratios of the $\Delta\delta$ values of α and β positions are about 0.5. Since the protons are separated from the lanthanide ions by four atoms at least, it is anticipated that the Fermi contact contribution to the paramagnetic shift is far smaller than the magnetic dipolar contribution. The dipolar contribution is proportional to a geometric factor $(3\cos^2\theta - 1)/(2R^3)$, where R is the distance between the paramagnetic center and the proton and θ is the azimuth of the proton with respect to the quantization axis, i.e., the C_4 axis. The geometric factors are fairly fixed for the six complexes. The fact that the ratios of $\Delta\delta$ values of α and β protons are near constant supports the presumption that the magnetic dipolar contribution is dominant.

Table 1. Assignments of ^{1}H NMR Signals δ and Paramagnetic Shifts $\Delta\delta$ for [Pc_2Ln]TBA

Ln	$\delta(\alpha)$	$\delta(\beta)$	$\Delta\delta(\alpha)$	$\Delta\delta(\beta)$	$\Delta\delta(\beta)/\Delta\delta(\alpha)$
Y	8.84	8.13			
Tb	−85.4	−40.58	−94.2	−48.71	0.52
Dy	−42.22	−18.38	−51.06	−26.51	0.52
Ho	−5.69	0.32	−14.53	−7.81	0.54
Er	35.05	21.17	26.21	13.04	0.50
Tm	34.83	21.20	25.99	13.07	0.50
Yb	11.89	9.69	3.05	1.56	0.51

In the earlier report on the ^{1}H NMR measurements on [Pc_2Ln]TBA,[15] there were oversights of signals lying in the negative region of chemical shift in the cases of Ln = Tb, Dy, and Ho. The conclusion in the paper that the Fermi contact contribution was significantly large,[15] therefore, has to be corrected. For the Er, Tm, and Yb cases, the signal assignments are basically unchanged.

Discussion

Determination of LF Parameters in the Lanthanide Complexes. In the previous papers,[1,2] we demonstrated that

substate structures of a series of lanthanide complexes having isomorphic structures can be determined by finding the set of the LF parameters that reproduce simultaneously the ^{1}H NMR paramagnetic shifts and the temperature dependence of magnetic susceptibilities. For the search of the LF parameters, any standard nonlinear multidimensional minimization algorithms can be used. In the present work, a simplex minimization method[16] was employed. We have searched for a set of LF parameters that gives the least-squares fit to $\chi_m T$ values at 2, 4, 8, 15, 30, 70, and 150 K, and the $\Delta\delta$ values of the α-proton of the six lanthanide systems.

The total angular momentum of the ground state in the trivalent lanthanide ions under consideration (f^8-f^{13}) is $J = L + S$. Each J state has $2J + 1$ sublevels in the ground-state multiplet. The Hamiltonian of a system under external magnetic field is

$$\hat{H} = \beta(\mathbf{L} + 2\mathbf{S})\cdot\mathbf{H} + \mathbf{F}$$

The first term of the right-hand side is the Zeeman effect. The orbital and spin angular momentum matrices, **L** and **S**, are those reconstructed so that the basis for the matrix elements is $|J,J_z\rangle$.

The second term is the LF interaction, which is expressed by the operator equivalent.[17] Following the notation by Abragam and Bleaney,[18] the LF term belonging to the C_4 point group is written as

$$\mathbf{F} = A_2^0\langle r^2\rangle\alpha\mathbf{O}_2^0 + A_4^0\langle r^4\rangle\beta\mathbf{O}_4^0 + A_4^4\langle r^4\rangle\beta\mathbf{O}_4^4 + A_6^0\langle r^6\rangle\gamma\mathbf{O}_6^0 + A_6^4\langle r^6\rangle\gamma\mathbf{O}_6^4$$

The coefficients $A_k^q\langle r^k\rangle$ are the parameters to be determined. The $\mathbf{O}_k^q$ matrices are polynomials of the total angular momentum matrices $\mathbf{J}^2$, $\mathbf{J}_z$, $\mathbf{J}_-$, and $\mathbf{J}_+$, and their definitions are described in ref 18. The z axis is chosen to coincide with the C_4 axis. The coefficients α, β, and γ are the constants tabulated by Stevens.[17] As in the previous attempts,[1,2] we employed an assumption that each parameter is expressed as a linear function of atomic number.

When the molecular symmetry is D_{4d}, where the two equivalent Pc rings are placed parallel to each other with a skew angle of 45°, $A_4^4\langle r^4\rangle$ and $A_6^4\langle r^6\rangle$ vanish. Since the angles in the Lu and Ho complexes are reported to be 45.0° and 43.2°,[11] the two LF parameters are expected to be small in the present cases. We performed the search with fixing the two parameters at zero. A separate calculation showed that improvement by moving the two parameters was negligible.

A set of $A_k^q\langle r^k\rangle$ coefficients and a finite external field determine the wave functions and magnetic moments of all the substates. The magnetization of an ensemble at a certain temperature is obtained considering Boltzmann distribution. The magnetic susceptibility per molecule is given by dividing the magnetization by the magnetic field applied. Thus, three principal values χ_{xx}, χ_{yy}, and χ_{zz} are obtained.

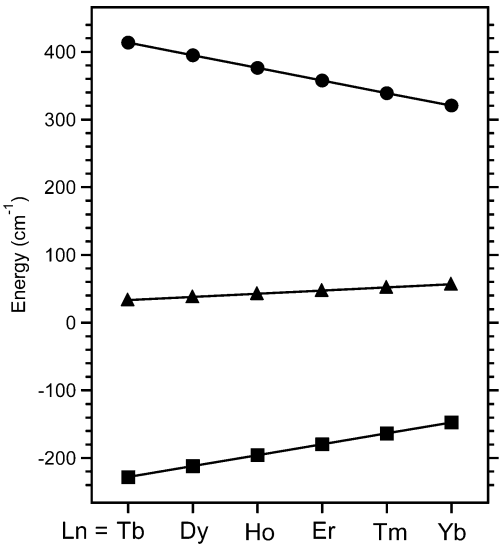

Figure 4. LF parameters $A_2^0\langle r^2\rangle$ (●), $A_4^0\langle r^4\rangle$ (■), and $A_6^0\langle r^6\rangle$ (▲) of [Pc_2Ln]TBA (Ln = Tb, Dy, Ho, Er, Tm, and Yb).

The observed molar magnetic susceptibility χ_m of a powder sample is

$$\chi_m = N_A\bar{\chi}$$

$$\bar{\chi} = \frac{1}{3}(\chi_{xx} + \chi_{yy} + \chi_{zz})$$

where N_A is the Avogadro number. Since the paramagnetic center of each molecule is placed in a ligand field of C_4 symmetry, the following relation is held.

$$\chi_{xx} = \chi_{yy}$$

The dipolar contribution in the ^{1}H NMR paramagnetic shift $\Delta\delta$ is written as

$$\Delta\delta = \frac{\Delta\nu}{\nu} = \frac{(3\cos^2\theta - 1)}{2R^3}(\chi_{zz} - \bar{\chi})$$

where ν is the resonance frequency in the reference diamagnetic molecule, $\Delta\nu$ is the change in the frequency in the paramagnetic molecule, R is the distance between the paramagnetic center and the proton to be considered, and θ is the corresponding azimuth.[19]

The R and θ values estimated from the X-ray crystal structures of [Pc_2Ln]TBA for Ln = Gd^{3+}, Ho^{3+}, and Lu^{3+} [11] indicate that deviation of the geometric factors ($3\cos^2\theta - 1$)/($2R^3$) from the averaged value is not negligible. To obtain the geometric factors for the f^8-f^{13} cases, we used a linear function of atomic number that gave the least-squares fit to the three values estimated from the X-ray structures.

Figure 4 shows the LF parameters thus obtained. The parameters give the best-fit $\chi_m T$ versus T plots shown in Figure 5 and paramagnetic shift $\Delta\delta$ values in Figure 6. The figures indicate that the obtained parameters reproduce both the SQUID and ^{1}H NMR data with good accuracy.

(16) Nelder, J. A.; Mead, R. *Comput. J.* **1965**, *7*, 308.
(17) Stevens, K. W. H. *Proc. Phys. Soc., London, Sect. A* **1952**, *65*, 209.
(18) Abragam, A.; Bleaney, B. *Electron Paramagnetic Resonance*; Clarendon Press: Oxford, 1970.
(19) Bleaney, B. *J. Magn. Reson.* **1972**, *8*, 91.

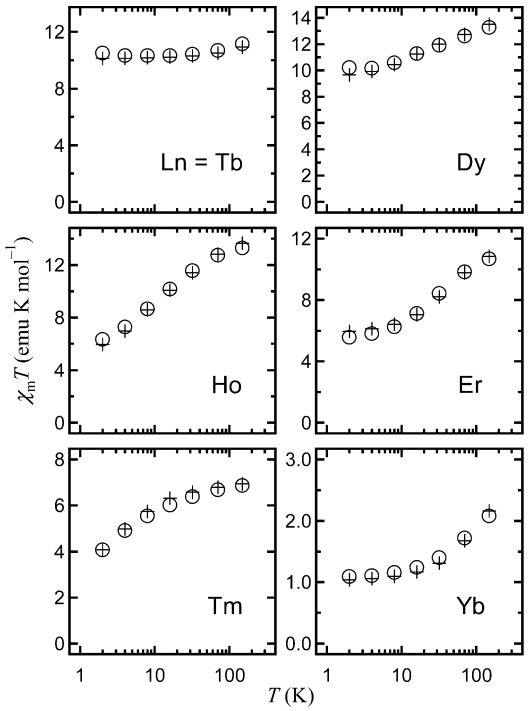

Figure 5. Theoretical temperature dependence of the $\chi_m T$ values (+) and the experimental data used for fitting (○) for [Pc_2Ln]TBA (Ln = Tb, Dy, Ho, Er, Tm, and Yb).

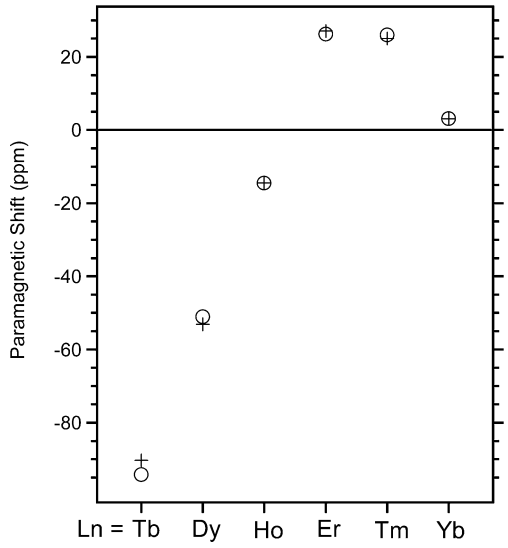

Figure 6. Theoretical (+) and observed (○) paramagnetic shifts of the ^{1}H NMR signal of the α-proton on the Pc ligands in [Pc_2Ln]TBA (Ln = Tb, Dy, Ho, Er, Tm, and Yb).

Electronic Structures of [Pc_2Ln]TBA. With the parameters determined as described, the electronic structures of the ground states of the six lanthanide systems are obtained. Figure 7 shows the energy levels of the $2J + 1$ sublevels of the ground state of each system.

(1) [Pc_2Tb]$^-$. The lowest substates are $|6\rangle$ and $|-6\rangle$, which have the largest J_z values within the $J = 6$ ground state (Table 2). This indicates the presence of a strong uniaxial magnetic anisotropy along the C_4 axis. The next sublevel lies at about 400 cm^{-1}. The large energy difference results in a predominant population of the lowest levels up to relatively high temperature: the population ratio remains 99.6% at 100 K,

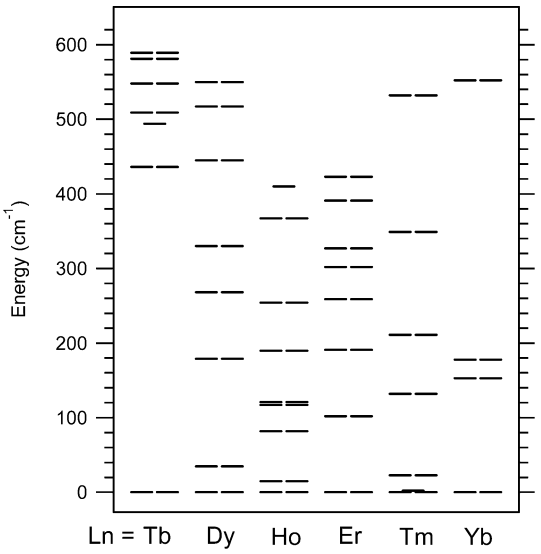

Figure 7. Energy diagram for the ground-state multiplets of [Pc_2Ln]$^-$ (Ln = Tb, Dy, Ho, Er, Tm, or Yb).

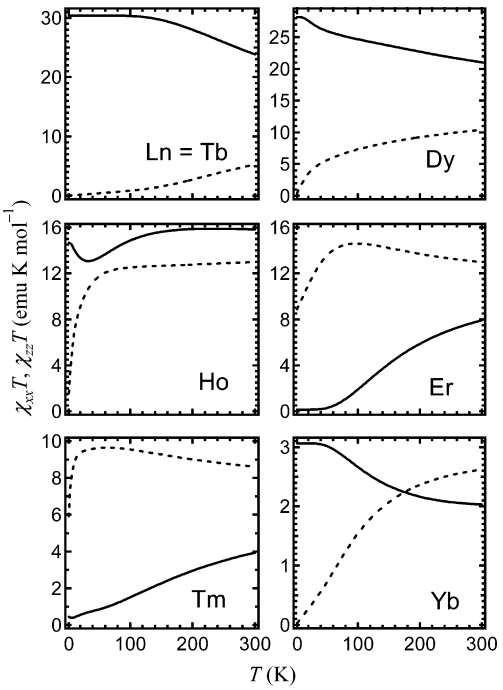

Figure 8. Theoretical temperature dependences of the products of the principal components of the magnetic susceptibilities and temperature, $\chi_{zz}T$ (—) and $\chi_{xx}T = \chi_{yy}T$ (- - -), of [Pc_2Ln]TBA.

Table 2. Energies and Wave Functions of the Ground-State Multiplets of [Pc_2Tb]$^-$

energy (cm^{-1})	wave function
0	$\|6\rangle$, $\|-6\rangle$
436	$\|5\rangle$, $\|-5\rangle$
494	$\|0\rangle$
509	$\|1\rangle$, $\|-1\rangle$
548	$\|2\rangle$, $\|-2\rangle$
581	$\|4\rangle$, $\|-4\rangle$
589	$\|3\rangle$, $\|-3\rangle$

at which point the χ_{zz} value starts decreasing (Figure 8). Static magnetic behavior of the complex below 100 K is almost exclusively described by the $|6\rangle$ and $|-6\rangle$ substates. At room temperature, the population of the lowest levels drops to 69%, which is still the largest number among the six lanthanide

Table 3. Energies and Wave Functions of the Ground-State Multiplets of $[Pc_2Dy]^-$

energy (cm^{-1})	wave function
0	$\|^{13}/_2\rangle$, $\|-^{13}/_2\rangle$
35	$\|^{11}/_2\rangle$, $\|-^{11}/_2\rangle$
179	$\|^{9}/_2\rangle$, $\|-^{9}/_2\rangle$
268	$\|^{15}/_2\rangle$, $\|-^{15}/_2\rangle$
330	$\|^{7}/_2\rangle$, $\|-^{7}/_2\rangle$
445	$\|^{5}/_2\rangle$, $\|-^{5}/_2\rangle$
517	$\|^{3}/_2\rangle$, $\|-^{3}/_2\rangle$
550	$\|^{1}/_2\rangle$, $\|-^{1}/_2\rangle$

Table 4. Energies and Wave Functions of the Ground-State Multiplets of $[Pc_2Ho]^-$

energy (cm^{-1})	wave function
0	$\|5\rangle$, $\|-5\rangle$
15	$\|4\rangle$, $\|-4\rangle$
82	$\|6\rangle$, $\|-6\rangle$
117	$\|3\rangle$, $\|-3\rangle$
121	$\|8\rangle$, $\|-8\rangle$
190	$\|7\rangle$, $\|-7\rangle$
254	$\|2\rangle$, $\|-2\rangle$
367	$\|1\rangle$, $\|-1\rangle$
410	$\|0\rangle$

Table 5. Energies and Wave Functions of the Ground-State Multiplets of $[Pc_2Er]^-$

energy (cm^{-1})	wave function
0	$\|^{1}/_2\rangle$, $\|-^{1}/_2\rangle$
102	$\|^{3}/_2\rangle$, $\|-^{3}/_2\rangle$
191	$\|^{13}/_2\rangle$, $\|-^{13}/_2\rangle$
259	$\|^{5}/_2\rangle$, $\|-^{5}/_2\rangle$
302	$\|^{15}/_2\rangle$, $\|-^{15}/_2\rangle$
327	$\|^{11}/_2\rangle$, $\|-^{11}/_2\rangle$
391	$\|^{7}/_2\rangle$, $\|-^{7}/_2\rangle$
423	$\|^{9}/_2\rangle$, $\|-^{9}/_2\rangle$

cases. The relatively slow variation of $\chi_{zz}T$ and $\chi_{xx}T$ is due to the large energy gap between the lowest substate and the second.

(2) $[Pc_2Dy]^-$. The lowest substates are $|^{13}/_2\rangle$ and $|-^{13}/_2\rangle$, J_z values of which are the second largest in the $J = {}^{15}/_2$ state (Table 3). The next substates $|^{11}/_2\rangle$ and $|-^{11}/_2\rangle$ lie at about 40 cm^{-1} above. Up to 10 K, the population to the $|\pm^{13}/_2\rangle$ state is more than 99%. The population drops to 73% at 50 K, while that of the $|\pm^{11}/_2\rangle$ level gains 27%. The relatively rapid change in $\chi_m T$ in the low temperature range is ascribed to the rapid increase of the population to the $|\pm^{11}/_2\rangle$ level.

(3) $[Pc_2Ho]^-$. The energy difference between the two lowest states is relatively small in this case. The $|\pm5\rangle$ states and the next $|\pm4\rangle$ states have intermediate J_z values in the $J = 8$ multiplets (Table 4). At 5 K, the population in the $|\pm5\rangle$ states is more than 99%, which decreases to 74% at 20 K, while $|\pm4\rangle$ states gain 25%. This rapid change in the population results in the large temperature dependences of $\chi_m T$ (Figure 2, bottom), $\chi_{zz}T$, and $\chi_{xx}T$ values at low temperatures.

(4) $[Pc_2Er]^-$. The lowest substates are $|^1/_2\rangle$ and $|-^1/_2\rangle$ with the smallest J_z in the $J = {}^{15}/_2$ multiplets (Table 5). This indicates the presence of a strong planar magnetic anisotropy at low temperature. The next sublevels are at relatively high energy. The contribution from the second lowest state $|\pm^3/_2\rangle$ becomes non-negligible at about 30 K, at which point the population of the state exceeds 0.7%.

Table 6. Energies and Wave Functions of the Ground-State Multiplets of $[Pc_2Tm]^-$

energy (cm^{-1})	wave function
0	$\|1\rangle$, $\|-1\rangle$
2	$\|0\rangle$
23	$\|2\rangle$, $\|-2\rangle$
132	$\|3\rangle$, $\|-3\rangle$
211	$\|6\rangle$, $\|-6\rangle$
349	$\|4\rangle$, $\|-4\rangle$
532	$\|5\rangle$, $\|-5\rangle$

Table 7. Energies and Wave Functions of the Ground-State Multiplets of $[Pc_2Yb]^-$

energy (cm^{-1})	wave function
0	$\|^5/_2\rangle$, $\|-^5/_2\rangle$
153	$\|^1/_2\rangle$, $\|-^1/_2\rangle$
178	$\|^3/_2\rangle$, $\|-^3/_2\rangle$
552	$\|^7/_2\rangle$, $\|-^7/_2\rangle$

(5) $[Pc_2Tm]^-$. The lowest sublevels are the nondegenerate $|0\rangle$ and degenerate $|\pm1\rangle$ (Table 6). A strong planar anisotropy is expected at low temperature because of the smallest J_z values of the substates in $J = 6$ multiplets. The calculated energy difference between the $|0\rangle$ and $|\pm1\rangle$ states is 2 cm^{-1}, which most probably falls within the experimental uncertainty. It is, therefore, not appropriate at this point to determine which state is really the lowest. The contribution from the third substate $|\pm2\rangle$ becomes significant from relatively low temperature: the population of the state exceeds 1% at 8 K.

(6) $[Pc_2Yb]^-$. The lowest substate is $|\pm^5/_2\rangle$ (Table 7). In the low temperature region, the predominant population to the state gives an axial magnetic anisotropy. As temperature rises, χ_{xx} increases and exceeds χ_{zz} at about 170 K. This conversion of the anisotropy from axial to planar is attributed to the increasing population to the next two substates $|\pm^3/_2\rangle$ and $|\pm^1/_2\rangle$.

Here it may be worthwhile to compare the multiplet splittings of the $[Pc_2Ln]^-$ to those of the Ln^{3+} ions doped in $LaCl_3$ matrix, which are often cited as the "standard" of lanthanide compounds. The symmetry of the crystal field that the $LaCl_3$ matrix gives is C_{3h}.[20] The energy differences from the lowest sublevel to the highest of the ground multiplets of Tb^{3+}, Dy^{3+}, Ho^{3+}, and Er^{3+} in a $LaCl_3$ matrix have been reported to be 118, 141, 213, and 229 cm^{-1}, respectively.[20] Each number is smaller than the corresponding value of $[Pc_2Ln]^-$. Aside from the question of whether the potentials with different symmetries can be compared directly or not, it may be safe to say that the strength of the ligand field in the bis(phthalocyaninato)lanthanides is greater than that in $LaCl_3$.

The successful convergence of the analysis strongly supports that paramagnetic shifts in $[Pc_2Ln]^-$ are determined predominantly by the magnetic dipolar term. Figure 9 shows the relation between the geometric parameter θ and the sign of the $\Delta\delta$ values. In Ln = Tb, Dy, and Ho cases, χ_{zz} is greater than χ_{xx} and χ_{yy} at room temperature. Since the protons of $[Pc_2Ln]^-$ are in the region $\theta > 54.7° = \arccos(3^{-1/2})$, a

(20) Dieke, G. H. *Spectra and Energy Levels of Rare Earth Ions in Crystals*; John Wiley & Sons: New York, 1968; Chapter 13.

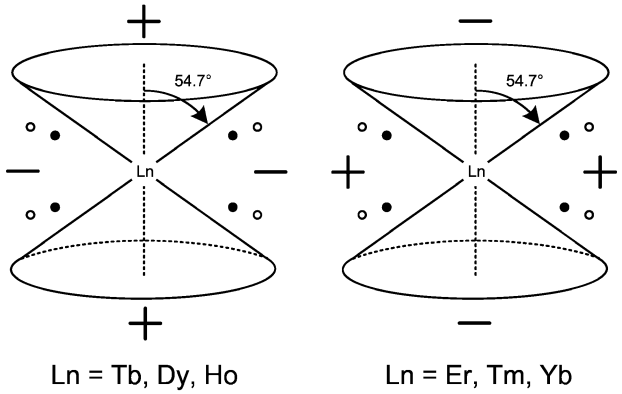

Figure 9. Relation between the geometric parameter θ and sign of the paramagnetic shifts of protons of $[Pc_2Ln]^-$. The black and white dots represent the position of α and β protons, respectively. The dotted lines are the 4-fold symmetric axis (*z* axis) of the complexes.

negative paramagnetic shift results from the dipolar contribution. On the other hand, in the Er, Tm, and Yb cases, χ_{zz} is smaller than χ_{xx} and χ_{yy} at room temperature, and therefore, positive dipolar shifts are observed.

Conclusions

We have elucidated the splitting structures of the ground-state multiplets of the six bis(phthalocyaninato)lanthanide complexes. It has been shown that a single set of LF parameters explains the diverse characteristics of the complexes observed in ^{1}H NMR paramagnetic shifts and the temperature dependences of the magnetic susceptibilities. The information on the f-electronic structures obtained here provides a firm theoretical foundation for further study of the properties in which f-electrons are associated, such as dynamical response to alternating magnetic field, magnetic anisotropies of single crystals, and f$-\pi$ interactions in the neutral Pc double-decker complexes.

Acknowledgment. This work was partially supported by Grant-in-Aid for Science Research 13740375 from the Ministry of Education, Science, Sports and Culture in Japan. The authors are greatly indebted to Prof. Toshiaki Enoki at the Tokyo Institute of Technology for making machine time available for the SQUID instrument. They also wish to thank to Dr. Akira Miyazaki and Dr. Kazuyuki Takai at the Tokyo Institute of Technology and Prof. Hirohiko Sato at the Chuo University for technical assistance, advice, and invaluable discussion in SQUID measurements.

IC026295U